Application of tensor decomposition theorems on DNS data of a viscoelastic material in the channel flow: understanding drag reduction mechanism

Roney L. Thompson, rthompson@mec.uff.br
Grupo de Escoamento de Fluidos Complexos - LMTA - PGMEC, Department of Mechanical Engineering, Universidade Federal Fluminense, Rua Passo da Pátria 156, Niteroi, RJ 24210-240, Brazil
Laurent Thais, laurent.thais@polytech.lille.fr
Gilmar Mompean, gilmar.mompean@polytech.lille.fr
Université des Science et Technologies de Lille, Polytech'Lille Laboratoire de Mécanique de Lille, UMR-CNRS 8107 Cité Scientifique, 59655 Villeneuve d'Ascq Cedex, France

Abstract. *An intriguing result which is not consensually explained is the drag reduction that occurs when a few ppm of a polymer with high molecular weight is added on a turbulent Newtonian flow. This problem deals with one of the most challenging subjects of Fluid Mechanics nowadays: turbulence of non-Newtonian fluids which combines complex phenomenon with complex material. It is consensual, however that the elasticity gained by the material by the addition of the polymer acts in a way that turbulence is inhibited and, therefore, drag is reduced. Here, data from a DNS calculation of a viscoelastic FENE-P material in the channel flow are used to understand some aspects of the mechanism of drag reduction. We first correlate the terms from the mean momentum equation that need closure models to the mean kinematic quantities such as* $\mathbf{D}$, $\mathbf{D}^2$ *and* $\mathbf{D}\cdot\left(\mathbf{W}-\mathbf{\Omega^D}\right)-\left(\mathbf{W}-\mathbf{\Omega^D}\right)\cdot\mathbf{D}$, *where* $\mathbf{D}$ *and* $\mathbf{W}$ *are, respectively, the symmetric and skew-symmetric parts of the velocity gradient and* $\mathbf{\Omega^D}$ *is the spin tensor related to the rotation of the eigenvectors of* $\mathbf{D}$. *These correlations are compared to the Newtonian case. After that, we correlate the conformation tensor (an average quantity that represents the main aspects of the configuration of a set of polymer molecules) to the anisotropic Reynolds stress and identify regions where these two tensors are in-phase and out-of-phase. The approach employed in the present work indicates a path to construct models for the turbulence of viscoelastic materials.*

Keywords: *Coherent structure, persistence-of-straining, vortex core, tensor decomposition, directional correlation*

1. INTRODUCTION

1.1 Turbulence of viscoelastic fluids

When a few parts per million of a polymeric material of a high molecular weight is added to a Newtonian turbulent flow, in a pipe for example, the drag reduces by large amount: 40%, 50%, sometimes up to 70%. This fact was verified in a number of experimental investigations and is well documented in Virk (1975). Although this phenomenon has been observed and verified, the true mechanism that leads to the drag reduction by polymer additives is still an open question. The results indicate, however, that only liquids with elastic properties are capable of producing a reduction on the drag. From some experimental data Virk et al. (1967, 1970) divided the domain in three sub-domains. Basically the viscous sub-layer and the turbulent core remain with the same features as the Newtonian ones. The difference occurs, mainly, at an intermediate layer where now there is a competition (not between inertial and viscous effects, as in the Newtonian case, but one) between elastic and viscous effects.

The theories presented by Lumley (1977) and Hinch (1977) are worth noting. They correlate the drag reduction phenomenon to an important rheological property of viscoelastic fluids: its extensional-thickening behavior. The turbulent flow does not exhibits a high correlation between the rate of angular deformation and the rate of linear deformation. Therefore, most of the polymer molecules, specially when they have long chains (in opposition to branched chains), can be oriented to the same direction for a long time. This kind of exposure to the main kinematics of the flow can highly distort the conformation of the molecule, and this characterizes a *strong flow*. In this case, the resistance to the extensional deformation, the extensional viscosity, can increase more then 10^4 times. This increase of resistant forces can alter dramatically the flow structure associated to the mechanisms of production and dissipation of turbulence which, at the end, changes the drag at the wall.

Since the theories to explain the drag reduction phenomenon are not consensual, investigations employing DNS calculations can be extremely helpful to understand the turbulence of viscoelastic liquids and, therefore, bring some light to this complex subject. It is worth noticing, however, that DNS simulations for viscoelastic liquids is philosophically different from its Newtonian counterpart. The reason for this difference is because the expression *Newtonian liquid* refers to a *real fluid* while the expression *FENE-P liquid*, for example, refers to a *model of a fluid*. This happens because there are liquids whose behavior, captured by measurements, adhere excellently to the hypothesis of a Newtonian constitutive model. On the other hand, there is no liquid which has an excellent degree of agreement to the hypothesis of an specific viscoelastic constitutive model.

In spite of these considerations, there has been some consistent studies using DNS simulations with viscoelastic

liquids in the last decade. The works of Massah and Haratty (1997), Sureskumar et al. (1997) and Dimitropoulos et al. (1998,2001) are of particular interest. They have used FENE-P and Giesekus models in their DNS simulations and found qualitative agreement with experimental results. The recent developments in DNS of viscoelastic models allow the reduction of the numerical diffusion due to formulations that are based on the evolution of the conformation tensor and, therefore higher level of Reynolds number were achieved. The investigations of Housiadas and Beris (2004a, 2004b) and Li et al. (2005) have found higher values of drag reduction, a consequence of the higher levels of Reynolds number, then the ones obtained previously.

In the present work DNS data for turbulent viscoelastic FENE-P model is filtered to find the part of the anisotropic Reynolds stress which is linear to the rate-of-strain tensor.

2. THEORETICAL ANALYSIS

2.1 Decomposition of a tensor with respect to another

2.1.1 General

Let us consider two second order tensors $\boldsymbol{\mathcal{U}}$ and $\boldsymbol{\mathcal{V}}$. There is a family of decompositions of tensor $\boldsymbol{\mathcal{V}}$ with respect to $\boldsymbol{\mathcal{U}}$ that is relevant in the present analysis. This family of decompositions decompose $\boldsymbol{\mathcal{V}}$ into two additive parts as

$$\boldsymbol{\mathcal{V}} = \boldsymbol{P}_{\boldsymbol{\mathcal{V}}}^{\boldsymbol{\mathcal{U}}} + \widetilde{\boldsymbol{P}}_{\boldsymbol{\mathcal{V}}}^{\boldsymbol{\mathcal{U}}} \tag{1}$$

that enjoy the following properties

i) $\boldsymbol{P}_{\boldsymbol{\mathcal{V}}}^{\boldsymbol{\mathcal{U}}}$ and $\widetilde{\boldsymbol{P}}_{\boldsymbol{\mathcal{V}}}^{\boldsymbol{\mathcal{U}}}$ are orthogonal[1].
ii) $\boldsymbol{\mathcal{U}}$ and $\boldsymbol{P}_{\boldsymbol{\mathcal{V}}}^{\boldsymbol{\mathcal{U}}}$ are coaxial[2]
iii) $\boldsymbol{\mathcal{U}}$ and $\widetilde{\boldsymbol{P}}_{\boldsymbol{\mathcal{V}}}^{\boldsymbol{\mathcal{U}}}$ are orthogonal.

If $\boldsymbol{\mathcal{U}}$ and $\boldsymbol{\mathcal{V}}$ were first order tensors, there would be an unique pair $\{\boldsymbol{P}_{\boldsymbol{\mathcal{V}}}^{\boldsymbol{\mathcal{U}}}, \widetilde{\boldsymbol{P}}_{\boldsymbol{\mathcal{V}}}^{\boldsymbol{\mathcal{U}}}\}$ that could satisfy properties (i)-(iii). Since $\boldsymbol{\mathcal{U}}$ and $\boldsymbol{\mathcal{V}}$ are second order tensors, these properties do not decompose $\boldsymbol{\mathcal{V}}$ in an unique manner. Essentially this happens because it is possible for a tensor to commute with and be orthogonal to a second tensor at the same time. A simple example that can illustrate this fact is the pair rate-of-strain tensor, $\mathbf{D}$, and the identity tensor, $\mathbf{1}$ for the case of an incompressible fluid. The identity tensor commutes with any other tensor and $\mathrm{tr}\,(\mathbf{D}\cdot\mathbf{I}) = \mathrm{tr}\mathbf{D} = 0$. Therefore, to construct the family of decompositions indicated, we can start from splitting tensor $\boldsymbol{\mathcal{V}}$ into three parts as

$$\boldsymbol{\mathcal{V}} = \boldsymbol{\varphi}_{\boldsymbol{\mathcal{V}}}^{\boldsymbol{\mathcal{U}}^{+}} + \boldsymbol{\varphi}_{\boldsymbol{\mathcal{V}}}^{\boldsymbol{\mathcal{U}}^{\pm}} + \boldsymbol{\varphi}_{\boldsymbol{\mathcal{V}}}^{\boldsymbol{\mathcal{U}}^{-}} \tag{2}$$

where $\boldsymbol{\varphi}_{\boldsymbol{\mathcal{V}}}^{\boldsymbol{\mathcal{U}}^{+}}$ is a part of $\boldsymbol{\mathcal{V}}$ that commutes with, but is not orthogonal to $\boldsymbol{\mathcal{U}}$, $\boldsymbol{\varphi}_{\boldsymbol{\mathcal{V}}}^{\boldsymbol{\mathcal{U}}^{\pm}}$ commutes with and is orthogonal to $\boldsymbol{\mathcal{U}}$, and $\boldsymbol{\varphi}_{\boldsymbol{\mathcal{V}}}^{\boldsymbol{\mathcal{U}}^{-}}$ does not commute with but is orthogonal to $\boldsymbol{\mathcal{U}}$. To enjoy the properties discriminated above, it can be shown that the quantities $\{\boldsymbol{P}_{\boldsymbol{\mathcal{V}}}^{\boldsymbol{\mathcal{U}}}, \widetilde{\boldsymbol{P}}_{\boldsymbol{\mathcal{V}}}^{\boldsymbol{\mathcal{U}}}\}$ obey the following relations

$$\boldsymbol{\varphi}_{\boldsymbol{\mathcal{V}}}^{\boldsymbol{\mathcal{U}}^{+}} \subseteq \boldsymbol{P}_{\boldsymbol{\mathcal{V}}}^{\boldsymbol{\mathcal{U}}} \subseteq \boldsymbol{\varphi}_{\boldsymbol{\mathcal{V}}}^{\boldsymbol{\mathcal{U}}^{+}} + \boldsymbol{\varphi}_{\boldsymbol{\mathcal{V}}}^{\boldsymbol{\mathcal{U}}^{\pm}} \tag{3}$$

$$\boldsymbol{\varphi}_{\boldsymbol{\mathcal{V}}}^{\boldsymbol{\mathcal{U}}^{-}} \subseteq \widetilde{\boldsymbol{P}}_{\boldsymbol{\mathcal{V}}}^{\boldsymbol{\mathcal{U}}} \subseteq \boldsymbol{\varphi}_{\boldsymbol{\mathcal{V}}}^{\boldsymbol{\mathcal{U}}^{-}} + \boldsymbol{\varphi}_{\boldsymbol{\mathcal{V}}}^{\boldsymbol{\mathcal{U}}^{\pm}} \tag{4}$$

In other words, uniqueness of the decomposition depends on a criterion of inclusion of tensor $\boldsymbol{\varphi}_{\boldsymbol{\mathcal{V}}}^{\boldsymbol{\mathcal{U}}^{\pm}}$, or parts of it, in each group $\boldsymbol{P}_{\boldsymbol{\mathcal{V}}}^{\boldsymbol{\mathcal{U}}}$ or $\widetilde{\boldsymbol{P}}_{\boldsymbol{\mathcal{V}}}^{\boldsymbol{\mathcal{U}}}$. The two extreme cases of this decomposition constitute the basis of the present analysis and are explored next.

2.1.2 Decoupling a tensor into a proportional and an orthogonal parts

In the scope of the present work, where turbulence modelling is considered, the analysis is carried out with the particular case where $\boldsymbol{\mathcal{U}}$ and $\boldsymbol{\mathcal{V}}$ are symmetric tensors. This is justified by the symmetry of the Reynolds stress and the kinematics tensors that compose the basis used to represent it. The first possible decomposition considered is when

$$\boldsymbol{P}_{\boldsymbol{\mathcal{V}}}^{\boldsymbol{\mathcal{U}}} = \boldsymbol{\Phi}_{\boldsymbol{\mathcal{V}}}^{\boldsymbol{\mathcal{U}}^{\neg\perp}} \equiv \boldsymbol{\varphi}_{\boldsymbol{\mathcal{V}}}^{\boldsymbol{\mathcal{U}}^{+}} \tag{5}$$

$$\widetilde{\boldsymbol{P}}_{\boldsymbol{\mathcal{V}}}^{\boldsymbol{\mathcal{U}}} = \boldsymbol{\Phi}_{\boldsymbol{\mathcal{V}}}^{\boldsymbol{\mathcal{U}}^{\perp}} \equiv \boldsymbol{\varphi}_{\boldsymbol{\mathcal{V}}}^{\boldsymbol{\mathcal{U}}^{\pm}} + \boldsymbol{\varphi}_{\boldsymbol{\mathcal{V}}}^{\boldsymbol{\mathcal{U}}^{-}} \tag{6}$$

where $\boldsymbol{\Phi}_{\boldsymbol{\mathcal{V}}}^{\boldsymbol{\mathcal{U}}^{\perp}}$ and $\boldsymbol{\Phi}_{\boldsymbol{\mathcal{V}}}^{\boldsymbol{\mathcal{U}}^{\neg\perp}}$ are, respectively the orthogonal and the non-orthogonal parts of $\boldsymbol{\mathcal{V}}$ related to $\boldsymbol{\mathcal{U}}$.

[1] Two tensors $\mathbf{A}$ and $\mathbf{B}$ are orthogonal if (and only if) $\mathrm{tr}\left(\mathbf{A}\cdot\mathbf{B}^{\mathrm{T}}\right) = 0$, where tr is the trace operator and the superscript T denotes transposition.
[2] Two tensors are coaxial if (and only if) they share the same eigenvectors. This condition is satisfied if (and only if) they commute.

This form of partition was employed by (e.g. Rajagopal and Srinivasa (2005)). Since every tensor commutes with itself, $\boldsymbol{\mathcal{U}}$ is part of the basis of tensors that are coaxial to itself. In other words we can write $\boldsymbol{\mathcal{V}}$ as

$$\boldsymbol{\mathcal{V}} = \varsigma \boldsymbol{\mathcal{U}} + \boldsymbol{\mathcal{W}} \tag{7}$$

Besides that, $\boldsymbol{\mathcal{U}}$ is a symmetric non-zero tensor and, therefore, it cannot be orthogonal to itself ($\mathrm{tr}\boldsymbol{\mathcal{U}}^2 \neq 0$). On the other hand, we can choose ς in such a way that $\boldsymbol{\mathcal{W}}$ is orthogonal to $\boldsymbol{\mathcal{U}}$. If we take the inner product of Eq.(7) with respect to tensor $\boldsymbol{\mathcal{U}}$ and impose $\mathrm{tr}\left(\boldsymbol{\mathcal{W}} \cdot \boldsymbol{\mathcal{U}}\right) = 0$ we have that

$$\varsigma = \frac{\mathrm{tr}\left(\boldsymbol{\mathcal{V}} \cdot \boldsymbol{\mathcal{U}}\right)}{\mathrm{tr}\left(\boldsymbol{\mathcal{U}} \cdot \boldsymbol{\mathcal{U}}\right)} = \frac{\boldsymbol{\mathcal{V}} : \boldsymbol{\mathcal{U}}}{\boldsymbol{\mathcal{U}} : \boldsymbol{\mathcal{U}}} \tag{8}$$

In the case of this decomposition, $\boldsymbol{P}_{\mathcal{V}}^{\mathcal{U}}$ is the part of $\boldsymbol{\mathcal{V}}$ that is proportional to $\boldsymbol{\mathcal{U}}$ or $\boldsymbol{P}_{\mathcal{V}}^{\mathcal{U}} = \varsigma \boldsymbol{\mathcal{U}}$.

2.1.3 Decoupling a tensor into a coaxial and an orthogonal parts

In Thompson (2008) a decomposition theorem was presented. Here we give a particular aspect of it as follows. Let us consider two second order symmetric tensors $\boldsymbol{\mathcal{U}}$ and $\boldsymbol{\mathcal{V}}$. Let us call $\mathbf{e}_i^{\mathcal{U}}$ and $\lambda_i^{\mathcal{U}}$ the (real) unit eigenvectors and eigenvalues of tensor $\boldsymbol{\mathcal{U}}$, respectively. Let us define a fourth order tensor $\mathbf{1}^{\mathcal{U}\mathcal{U}}$ as

$$\mathbf{1}^{\mathcal{U}\mathcal{U}} = \sum_{k=1}^{3} \mathbf{e}_k^{\mathcal{U}} \mathbf{e}_k^{\mathcal{U}} \mathbf{e}_k^{\mathcal{U}} \mathbf{e}_k^{\mathcal{U}} \tag{9}$$

and a decomposition of tensor $\boldsymbol{\mathcal{V}}$, such that

$$\boldsymbol{\mathcal{V}} = \boldsymbol{\Phi}_{\mathcal{V}}^{\mathcal{U}} + \widetilde{\boldsymbol{\Phi}}_{\mathcal{V}}^{\mathcal{U}} \tag{10}$$

where

$$\boldsymbol{\Phi}_{\mathcal{V}}^{\mathcal{U}} = \mathbf{1}^{\mathcal{U}\mathcal{U}} : \boldsymbol{\mathcal{V}} \tag{11}$$

$$\widetilde{\boldsymbol{\Phi}}_{\mathcal{V}}^{\mathcal{U}} = \left(\mathbf{1}^{\delta\delta} - \mathbf{1}^{\mathcal{U}\mathcal{U}}\right) : \boldsymbol{\mathcal{V}} \tag{12}$$

and $\mathbf{1}^{\delta\delta}$ is the fourth order identity tensor that when applied to any second order tensor maps this tensor to itself, as follows

$$\mathbf{1}^{\delta\delta} : \boldsymbol{B} = \boldsymbol{B} \tag{13}$$

In this case, from Eqs.(3) and (4) we can identify

$$\boldsymbol{P}_{\mathcal{V}}^{\mathcal{U}} = \boldsymbol{\Phi}_{\mathcal{V}}^{\mathcal{U}} = \boldsymbol{\varphi}_{\mathcal{V}}^{\mathcal{U}^+} + \boldsymbol{\varphi}_{\mathcal{V}}^{\mathcal{U}^\pm} \tag{14}$$

$$\widetilde{\boldsymbol{P}}_{\mathcal{V}}^{\mathcal{U}} = \widetilde{\boldsymbol{\Phi}}_{\mathcal{V}}^{\mathcal{U}} = \boldsymbol{\varphi}_{\mathcal{V}}^{\mathcal{U}^-} \tag{15}$$

Then, the decomposition given by Eqs.(10), (11), and (12) have, besides properties (i)-(iii), the following ones

- $\boldsymbol{\mathcal{U}} : \boldsymbol{\mathcal{V}} = \boldsymbol{\mathcal{U}} : \boldsymbol{\Phi}_{\mathcal{V}}^{\mathcal{U}}$
- $\widetilde{\Xi}\left[\boldsymbol{\mathcal{U}}, \boldsymbol{\mathcal{V}}\right] = \widetilde{\Xi}\left[\boldsymbol{\mathcal{U}}, \widetilde{\boldsymbol{\Phi}}_{\mathcal{V}}^{\mathcal{U}}\right]$

where the second order tensor-valued function $\widetilde{\Xi}\left[\boldsymbol{\mathcal{U}}, \boldsymbol{\mathcal{V}}\right]$ denotes the Lie product between any two second order tensors, defined as

$$\widetilde{\Xi}\left[\boldsymbol{\mathcal{U}}, \boldsymbol{\mathcal{V}}\right] \equiv \boldsymbol{\mathcal{U}} \cdot \boldsymbol{\mathcal{V}} - \boldsymbol{\mathcal{V}} \cdot \boldsymbol{\mathcal{U}} \tag{16}$$

In a matrix form Eq.(10) is written as

$$\left[\boldsymbol{\mathcal{V}}^{\mathcal{U}}\right] = \begin{bmatrix} \mathcal{V}_{11}^{\mathcal{U}} & \mathcal{V}_{12}^{\mathcal{U}} & \mathcal{V}_{13}^{\mathcal{U}} \\ \mathcal{V}_{21}^{\mathcal{U}} & \mathcal{V}_{22}^{\mathcal{U}} & \mathcal{V}_{23}^{\mathcal{U}} \\ \mathcal{V}_{31}^{\mathcal{U}} & \mathcal{V}_{32}^{\mathcal{U}} & \mathcal{V}_{33}^{\mathcal{U}} \end{bmatrix} = \begin{bmatrix} \mathcal{V}_{11}^{\mathcal{U}} & 0 & 0 \\ 0 & \mathcal{V}_{22}^{\mathcal{U}} & 0 \\ 0 & 0 & \mathcal{V}_{33}^{\mathcal{U}} \end{bmatrix} + \begin{bmatrix} 0 & \mathcal{V}_{12}^{\mathcal{U}} & \mathcal{V}_{13}^{\mathcal{U}} \\ \mathcal{V}_{21}^{\mathcal{U}} & 0 & \mathcal{V}_{23}^{\mathcal{U}} \\ \mathcal{V}_{31}^{\mathcal{U}} & \mathcal{V}_{32}^{\mathcal{U}} & 0 \end{bmatrix} \tag{17}$$

Because of the above properties, tensors $\boldsymbol{\Phi}_{\mathcal{V}}^{\mathcal{U}}$ and $\widetilde{\boldsymbol{\Phi}}_{\mathcal{V}}^{\mathcal{U}}$ were called (Thompson (2008)) the *in-phase* and *out-of-phase* parts of $\boldsymbol{\mathcal{V}}$ with respect to $\boldsymbol{\mathcal{U}}$. The following properties are important in the present context

1. When tensors $\boldsymbol{\mathcal{U}}$ and $\boldsymbol{\mathcal{V}}$ commute, $\boldsymbol{\Phi}_{\mathcal{V}}^{\mathcal{U}} = \boldsymbol{\mathcal{V}}$ and $\widetilde{\boldsymbol{\Phi}}_{\mathcal{V}}^{\mathcal{U}} = \mathbf{0}$.
2. When $\boldsymbol{\mathcal{V}} = \mathbf{A}^S \cdot \mathbf{B}^W - \mathbf{B}^W \cdot \mathbf{A}^S$, where $\mathbf{A}^S$ is symmetric tensor which commutes with $\boldsymbol{\mathcal{U}}$ and $\mathbf{B}^W$ is skew-symmetric, $\boldsymbol{\Phi}_{\mathcal{V}}^{\mathcal{U}} = \mathbf{0}$ and $\widetilde{\boldsymbol{\Phi}}_{\mathcal{V}}^{\mathcal{U}} = \boldsymbol{\mathcal{V}}$.

It is worth noting that since $\boldsymbol{\Phi}_{\mathcal{V}}^{\mathcal{U}}$ and $\widetilde{\boldsymbol{\Phi}}_{\mathcal{V}}^{\mathcal{U}}$ are orthogonal (or uncorrelated), the norm of $\boldsymbol{\mathcal{V}}$, $\|\boldsymbol{\mathcal{V}}\| = \sqrt{\boldsymbol{\mathcal{V}} \cdot \boldsymbol{\mathcal{V}}^T}$ is given by

$$\sqrt{\boldsymbol{\mathcal{V}} \cdot \boldsymbol{\mathcal{V}}^T} = \sqrt{\left(\boldsymbol{\Phi}_{\mathcal{V}}^{\mathcal{U}} + \widetilde{\boldsymbol{\Phi}}_{\mathcal{V}}^{\mathcal{U}}\right) \cdot \left(\boldsymbol{\Phi}_{\mathcal{V}}^{\mathcal{U}} + \widetilde{\boldsymbol{\Phi}}_{\mathcal{V}}^{\mathcal{U}}\right)^T} = \sqrt{\|\boldsymbol{\Phi}_{\mathcal{V}}^{\mathcal{U}}\|^2 + \|\widetilde{\boldsymbol{\Phi}}_{\mathcal{V}}^{\mathcal{U}}\|^2} \tag{18}$$

A normalized parameter that measures how tensor $\boldsymbol{\mathcal{V}}$ is in-phase with tensor $\boldsymbol{\mathcal{U}}$ can be constructed by the relation

$$\widehat{\Phi}_{\mathcal{V}}^{\mathcal{U}} = 1 - \frac{2}{\pi} \cos^{-1}\left(\frac{\|\boldsymbol{\Phi}_{\mathcal{V}}^{\mathcal{U}}\|}{\|\boldsymbol{\mathcal{V}}\|}\right) \tag{19}$$

$\widehat{\Phi}_{\mathcal{V}}^{\mathcal{U}} \in [0, 1]$, where $\widehat{\Phi}_{\mathcal{V}}^{\mathcal{U}} = 0$ being the case where $\boldsymbol{\mathcal{U}}$ and $\boldsymbol{\mathcal{V}}$ are uncorrelated and $\widehat{\Phi}_{\mathcal{V}}^{\mathcal{U}} = 1$ when $\boldsymbol{\mathcal{U}}$ and $\boldsymbol{\mathcal{V}}$ are coaxial, i.e. share the same eigenvectors.

2.2 The approach of the present analysis

The Reynolds stress tensor, $\mathbf{R}$, is defined through

$$\mathbf{R} = \overline{u_i' u_j'} \mathbf{e}_i \mathbf{e}_j \tag{20}$$

where u_i' are fluctuations of the i-component of the velocity and the overline, $\overline{()}$ indicates the average operation. The Boussinesq hypothesis (Boussinesq (1877)), is based on the the assumption that the turbulent shear stress is linearly dependent on the velocity gradient. Therefore the structure of the relation between molecular shear stress and kinematics is maintained for the turbulent shear stress. Hence, for a 2-D cartesian flow where x is the coordinate along the wall and y is orthogonal to this wall

$$-\overline{u'v'} = \nu_T \frac{\partial U}{\partial y} \tag{21}$$

where ν_T is a "turbulent viscosity".

The generalization of this hypothesis was done by Komolgorov (1942). Let us considered tensor $\mathbf{b}$, the anisotropic Reynolds stress defined as

$$\mathbf{b} = -\left(\mathbf{R} - \frac{1}{3}\mathrm{tr}\mathbf{R}\right) \tag{22}$$

Therefore, a tensor version of Eq.(21) can be written as

$$\mathbf{b} = 2\nu_T \mathbf{D} \tag{23}$$

where $\mathbf{D}$ is the symmetric part of the mean velocity gradient. Let us suppose we have obtained the Reynolds stress (and therefore $\mathbf{b}$) from a DNS or experimental data. Let us suppose this same source has provided us with some kinematic information such as the velocity profile. Therefore, one can calculate $\mathbf{D}$. How can we test if Eq.(23) holds? Or, what is a better approach, how can we quantify how Eq.(23) adheres to the data in a general flow? And how can we obtain ν_T?

The approach used here, in this first analysis is to decompose tensor $\mathbf{b}$ into a tensor which is proportional to $\mathbf{D}$ and a tensor which is orthogonal to $\mathbf{D}$, $\mathbf{D}^\perp$. Hence,

$$\mathbf{b} = \alpha \mathbf{D} + \beta \mathbf{D}^\perp \tag{24}$$

If we take the inner product of Eq.(24) with respect to $\mathbf{D}$ and impose that $\mathrm{tr}\left(\mathbf{D}^\perp \cdot \mathbf{D}\right) = 0$, we have that

$$\alpha = \frac{\mathrm{tr}\left(\mathbf{b} \cdot \mathbf{D}\right)}{\mathrm{tr}\left(\mathbf{D} \cdot \mathbf{D}\right)} \tag{25}$$

Therefore, α is the best scalar that can be related to the turbulent viscosity defined by Eq.(23). The idea here is to present this scalar in the usual dimensionless form (C_μ) where the kinetic energy and dissipation are used to compose a quantity with the viscosity dimension. Therefore

$$\alpha = 2C_\mu \frac{k^2}{\epsilon} \tag{26}$$

An important index of the present analysis is a global measure of how important is the term $\alpha\mathbf{D}$ when compared to $\mathbf{b}$, in other words, how Komolgorov's Eq.(23) can fit DNS or experimental data.

Based on Eq. (19), this parameter, $index_I$, is given by

$$index_I = 1 - \frac{2}{\pi}\cos^{-1}\left(\sqrt{\frac{\mathrm{tr}\,(\alpha^2\mathbf{D}^2)}{\mathrm{tr}\,\mathbf{b}^2}}\right) \tag{27}$$

and, by construction, $index_I$ is a normalized parameter ($index_I \in [0,1]$)

3. DNS DATA

The channel flow direct numerical simulations (DNS) were conducted in a rectangular channel at an imposed moderate zero-shear frictional Reynolds number $Re_\tau = 180$, corresponding to a Newtonian bulk Reynolds number $Re_{bulk} = 2800$ based on the channel half-height h. The channel size is $L_x = 4\pi h$, $L_y = 2h$, $L_z = 4/3\pi h$. In the homogeneous directions, these amount to $L_x+ \simeq 2300$ and $L_y+ \simeq 750$ in wall units.

The DNS grid has $128 \times 129 \times 128$ points in the respective streamwise, wall-normal, and spanwise directions, i.e. $\Delta x_+ \simeq 17$ and $\Delta z_+ \simeq 6$ in the homogeneous directions. The grid in the wall-normal direction has a tanh distribution such that $0.2 \leq \Delta y_+ \leq 7$ and incorporates about 20 points in the first 10 wall units, which is enough to resolve the smallest turbulent structures in the near wall region. The time step used on this grid is $\Delta \mathrm{t} = 0.001\, h/u_{ave}$.

The non-Newtonian version of the numerical code which was developed for the present study is a direct extrapolation of the code described in detail by Tejada-Martínez and Grosch (2007). The code uses the Message Passing Interface protocol following the same parallel structure presented by Winters et al. (2004). Only a brief description will be given below. The momentum equations are solved with a hybrid spectral finite-difference scheme. A two-dimensional Fourier-spectral discretization is used in the homogeneous directions (x, z) whereas 6-th order compact finite difference formuli are used in the wall-normal direction y (Lele Carpenter (1992)), downgraded to 5-th order at the first two boundary points (Carpenter (1993)). The time advancement of the solution consisted of the second order time-accurate pressure correction scheme on a non-staggered grid analyzed by Armfield and Street (2000). This procedure uses the implicit mid-point trapezoidal rule for viscous terms and the explicit second-order accurate Adams-Bashforth rule for advection. Furthermore, the three half rule is used for de-aliasing all the non-linear terms, along each one of the periodic directions. The boundary conditions for the conformation tensor are imposed following the guidelines of Sureskumar et al. (2001). The conformation tensor equations without artificial difusivity are first updated right at the top and the bottom boundaries of the channel. These values are then used as boundary conditions to step forward the full conformation tensor equations (including artificial diffusivity). This scheme proves stable provided a sufficient amount of artificial stress diffusivity imposed.

4. PRELIMINARY RESULTS

The instantaneous dissipation was computed during the first half of the DNS simulations and the average was taken from that point. The kinetic energy was computed after the hole simulation, as a post-processing quantity. A general result is the production over dissipation $\left(\frac{P}{\epsilon}\right)$ as a function of position in wall units. This is presented on Fig.(1). Here we can see a continuously behavior as elastic effects are increased. There is a peak where the dissipation is minimum and also a beginning of plateau where production and dissipation reach an equilibrium. After a certain value of y^+, the power of the flow, due to its low Reynolds number makes the production to diminish its strength till the center of the channel where there is no production.

4.1 Analysis of the part of the Reynolds stress tensor which is linear with the rate-of-strain

The result concerning a dimensionless viscosity coefficient, C_μ, as stated by Eq.(25) is shown in Fig.(2). We can also see a tendency of the general behavior of the fluid as elasticity is increased. There is a peak and, after that, C_μ decreases monotonically till a certain value near the center of the channel.

Figure (3) shows the profile of $index_I$, the importance of $\alpha\mathbf{D}$ on the Reynolds stress tensor, as given by Eq.(27). We can see that the maximum value decreases as elasticity increases.

5. FINAL REMARKS

The general results obtained show that as elasticity increases the part of the Reynolds stress that is proportional to $\mathbf{D}$ decreases. Further investigation is needed.

6. ACKNOWLEDGEMENTS

We would like to acknowledge CNPq, CNRS, and FAPERJ for financial support.

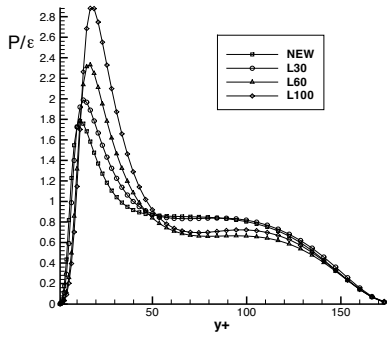

Figure 1. Production over dissipation.

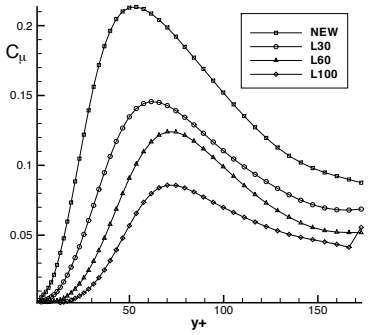

Figure 2. Dimensionless viscosity coefficient.

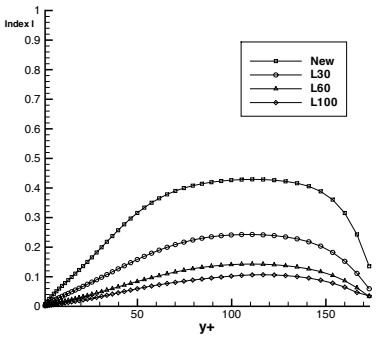

Figure 3. Index I, a measure of the hypothesis that the Reynolds stress tensor is a linear function of $\mathbf{D}$.

7. REFERENCES

Armfield, S., Street, R., 2000. Fractional step methods for the navier-stokes equations on non-staggered grids. ANZIAM J. 42(E), C134–C156.

Boussinesq, M., 1877. Essai sur la thet'orie des eaux courantes. Imprimerie Nationale, Paris XXIII.

Carpenter, M., 1992. Compact finite difference schemes with spectral-like resolution. J. Comp. Phys. 103(1), 16–42.

Carpenter, M., 1993. The stability of numerical boundary treatments for compact high-order finite-difference schemes. J. Comp. Phys. 108(2), 272–295.

Rajagopal, K., Srinivasa, A., 2005. On the nature of constraints for continua undergoing dissipative processes. Proc. R. Soc. Lond. A 461, 2785–2795.

Tejada-Martínez, A., Grosch, C., 2007. Langmuir turbulence in shallow water: part ii. large eddy simulations. J. Fluid Mech. 576, 63–108.

Thompson, R. L., 2008. Some perspectives on the dynamic history of a material element. Int. J. Engng. Sci 46, 524–549.

Winters, K., MacKinnon, J., Mills, B., 2004. A spectral model for process studies of rotating, density-stratified flows. J. of Atmospheric and Oceanic Technology. 21(1), 69–94.

8. Responsibility notice

The author(s) is (are) the only responsible for the printed material included in this paper